Supporting Information

Implementing Lateral $MoSe_2$ P-N Homo-junction by Efficient Carrier Type Modulation

*[1]Shuangqing Fan, [1]Wanfu Shen, [1]Chunhua An, [1]Zhaoyang Sun, [1]Sen Wu, [1]Linyan Xu, [2]Dong Sun, [1]Xiaodong Hu, [1]Daihua Zhang and [1]Jing Liu**

[1]State Key Laboratory of Precision Measurement Technology and Instruments, School of Precision Instruments and Opto-electronics Engineering

Tianjin University, No. 92 Weijin Road, Tianjin, 300072, China

[2]International Center for Quantum Materials, School of Physics, Peiking University, No. 5 Yiheyuan Road, Beijing 100871, China

Corresponding author e-mail: jingliu_1112@tju.edu.cn

Optical microscopy image of the $MoSe_2$ FET

The $MoSe_2$ was mechanically exfoliated on to SiO_2/Si substrate and electron beam lithography was subsequently employed to pattern electrodes, followed by the deposition of 10 nm Cr and 30 nm Au as metal contacts. The electrode 2 and 3 were used as source and drain electrodes, respectively. We tested the $MoSe_2$ FET before and after annealing for various durations at 360 ^{o}C in air environment as shown in Fig. 1(a-c).

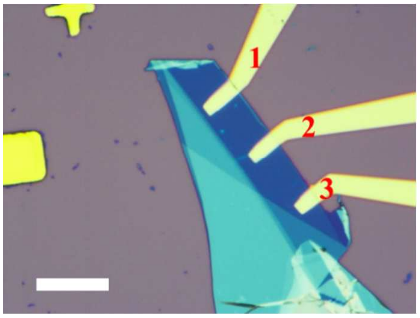

Figure S1. Optical microscopy image of the $MoSe_2$ FET. Scale bar is 10 μm.

Effects of atmospheric exposure on the electrical properties of annealed $MoSe_2$

As the exposure time increases, the off current of the annealed MoSe2 FET decreases from 10^{-8} A to 10^{-11} A. This may be due to the adsorption of gas molecular such as oxygen and

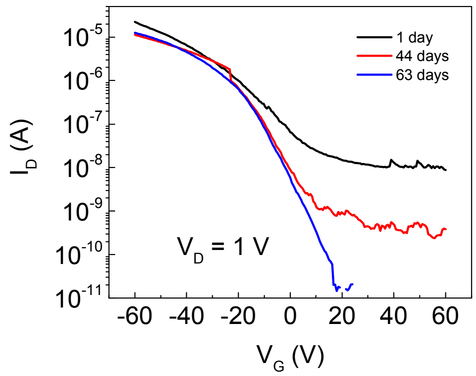

water on the surface of the $MoSe_2$.

Figure S2. Transfer curves of an annealed $MoSe_2$ FET after being exposed in atmospheric environment for 1, 44 and 63 days.

Temperature-dependent p-type modulation of the $MoSe_2$ FET

Generally, as the annealing temperature increases, the n-branch current of the $MoSe_2$ FET decreases, while the p-branch current increases. However, when the temperature increases to

390 ^{o}C, the on-state current and on/off ratio both decreases as compared to that at 360 ^{o}C. Hence, we chose the 360 ^{o}C as the optimum temperature tp p-type dope $MoSe_2$. The linear-scale curves are shown in Fig. 2a.

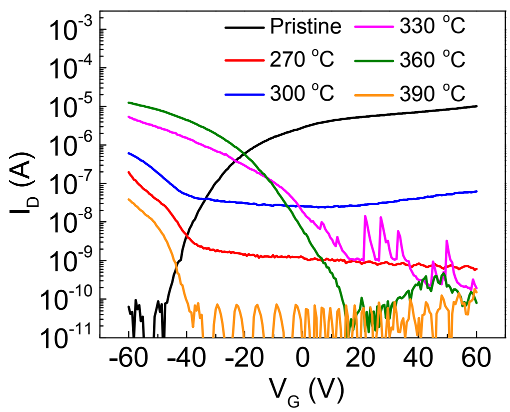

Figure S3. Semi-log scale I_D-V_G curves of $MoSe_2$ FETs in a pristine state and after being treated by air RTA under various temperatures.

$MoSe_2$ thickness effect on RTA process

When the thickness is equal to or greater than 4.2 nm, the $MoSe_2$ can be successfully p-doped by annealing. In contrast, when the thickness is less than 2.1 nm (~4 layers), the channel current of $MoSe_2$ FET is cut off, which may be due to the disruption of the $MoSe_2$ lattice. Therefore, the thickness of $MoSe_2$ should be equal to or greater than 4.2 nm to be successfully p-doped by annealing. The associated hole mobility of the annealed $MoSe_2$ with different thicknesses is also presented in Fig. S4m, which decreases as a function of the thickness.

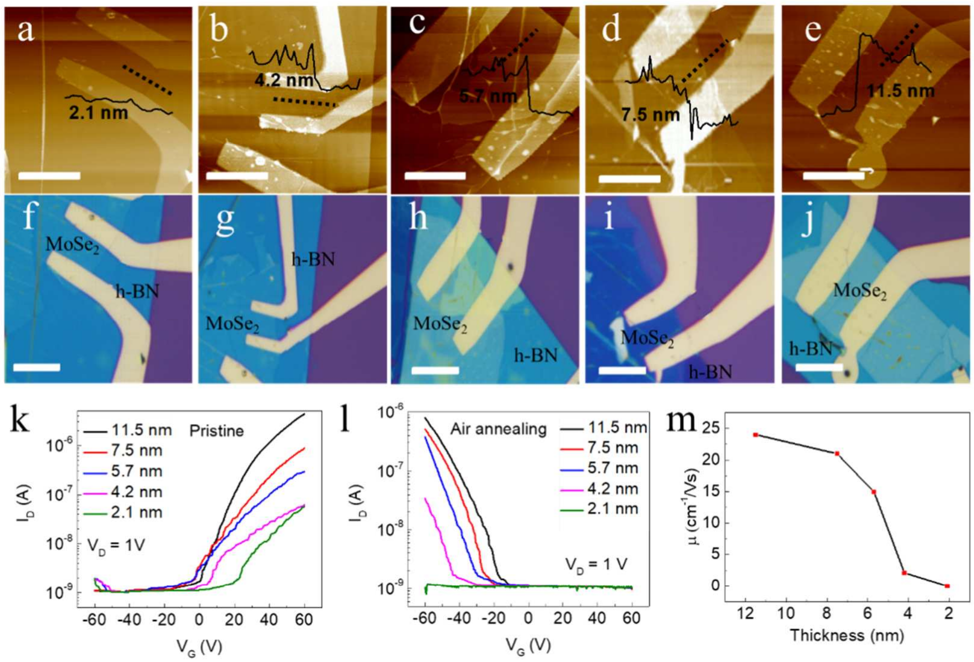

Figure S4. (a-e) AFM and (f-j) optical images of $MoSe_2$ flakes with thickness ranging from 2.1 nm to 11.5 nm. Scale bars are 5 μm. We first mechanically exfoliated h-BN (5~10 nm) onto SiO_2/Si substrate, and then transfer $MoSe_2$ with various thickness on h-BN, followed by depositing source and drain electrodes. (k, l) Transfer characteristics of these $MoSe_2$ FETs before (k) and after (l) annealing for 4 min under 360 ^oC. (m) Hole mobility of the MoSe2 FET as a function of flake thickness after annealing.

HR-TEM images of a $MoSe_2$ flake before and after air annealing

It can be seen from the images that the $MoSe_2$ flake exhibits hexagonal phase both before and after annealing, indicating that air annealing has limited impact on the lattice structure of $MoSe_2$.

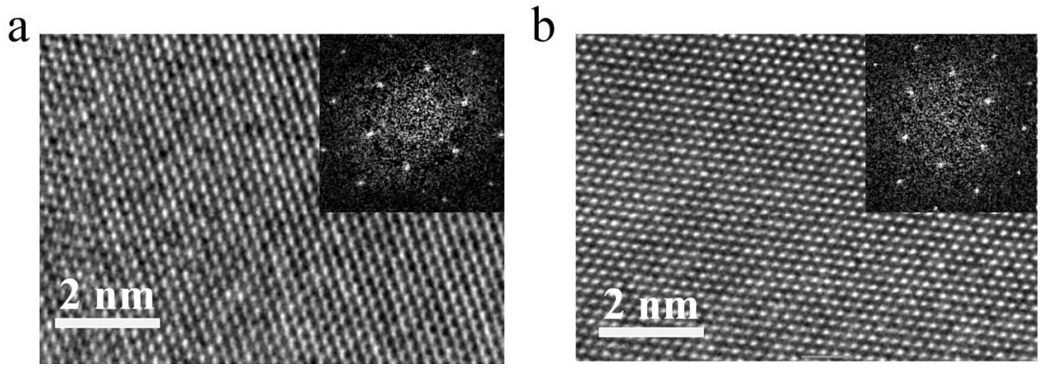

Figure S5. (a,b) High resolution TEM images of an $MoSe_2$ flake before (a) and after(b) annealing under 360 ^oC in air for 4 min. The insets in (a,b) are FFT patterns from the entire area of (a,b).

<u>XPS surveys of $MoSe_2$ before and after air annealing</u>

According to the XPS surveys and zoomed-in C1s core levels, no additional signals are found after annealing, indicating that the moisture and carbon species have limited affect.

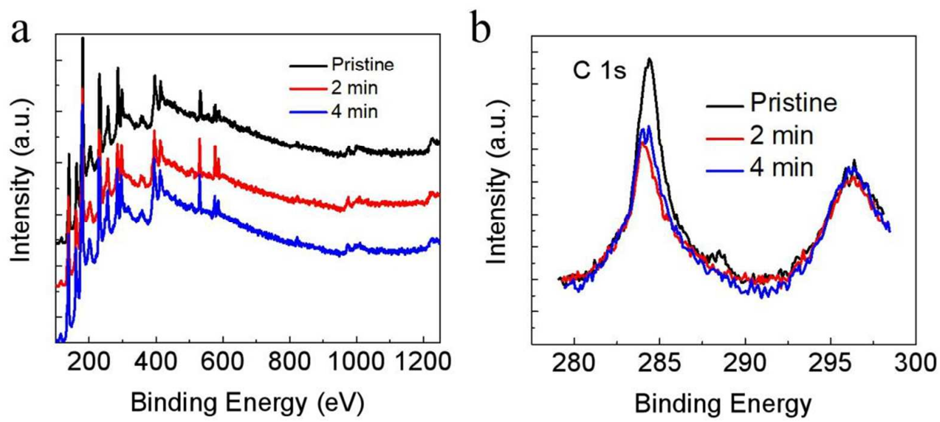

Figure S6. (a) Extended and (b) zoomed-in (at C1s core level) XPS spectra of $MoSe_2$ sample before and after annealing for 2 min and 4 min, respectively.

<u>Electron density and mobility of $MoSe_2$ FET n-doped by PPh_3</u>

As the PPh_3 concentration increases from 0 mM to 30 mM, electron mobility μ_n increases from 78.6 to 412.8 $cm^2\ V^{-1}\ s^{-1}$ and electron density n_e increases from 8.8×10^{11} to 9.0×10^{12} cm^{-2}.

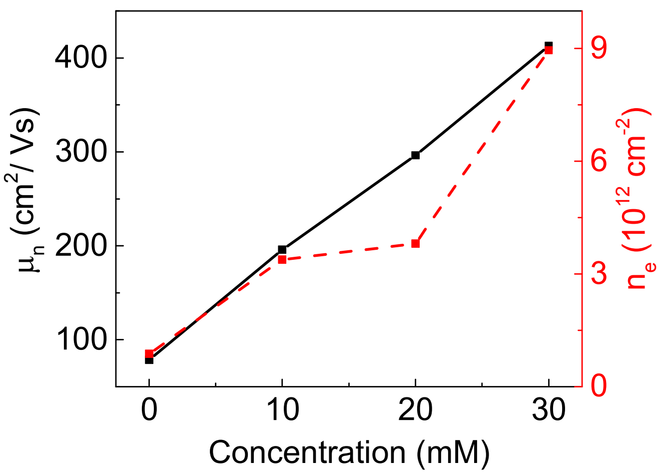

Figure S7. Plot of extracted n_e at V_G = 60 V and μ_n as a function of PPh_3 concentration.

Intensity-dependent dynamic photo-response of $MoSe_2$ homo-junction

The illumination light intensity ranges from 0.01 to 2.5 mW·cm^{-2} with the wavelength mixed at 532 nm. The gate and source-drain bias is 0 V.

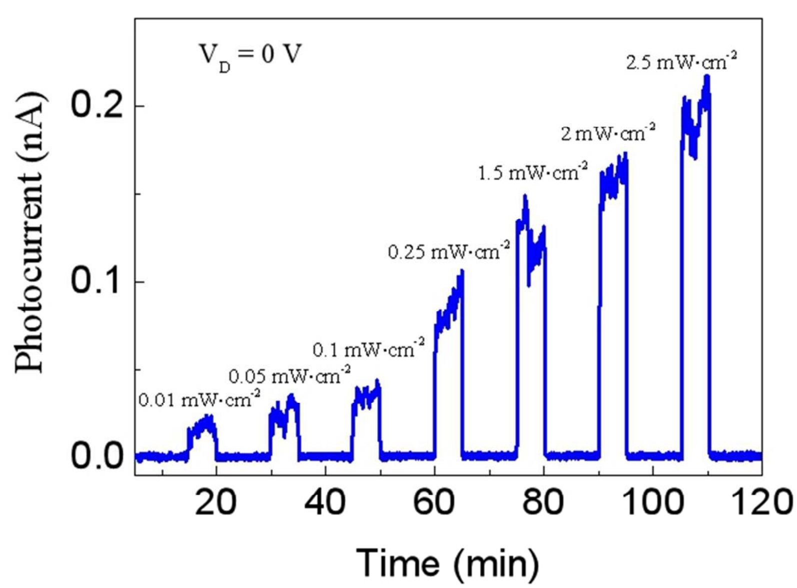

Figure S8. Intensity-dependent photo-response of the $MoSe_2$ homo-junction.